analytical chemistry

ARTICLE

pubs.acs.org/ac

Multifunctional Encoded Self-Assembling Protein Nanofibrils as Platform for High-Throughput and Multiplexed Detection of Biomolecules

Ho-Man Chan and Hung-Wing Li*

Department of Chemistry, Hong Kong Baptist University, Kowloon Tong, Hong Kong, People's Republic of China

Supporting Information

ABSTRACT: A one-dimensional nanofibrillar array formed by the co-assembly of native and biotin-functionalized beta-amyloid (Aβ) peptide was developed for biomolecule sensing. With the presence of biotin moiety, a variety of biomolecular probes can be conjugated onto the nanofibrils, thus converting the protein assembly into a miniature biosensor. In this work, DNA probes were immobilized onto the fibril for the detection of cDNA sequences. The as-developed "DNA-nanoarray" achieved a detection limit at subattomole level (183 fM in 10 μL). This highly sensitive, yet simple, assay requires a trace amount of sample consumption (<10 μL) and is pretreatment-free. In addition, we reported the preparation of alternate-segmented amyloid nanofibrils with multifunctionality. The fibrils hereby serve as an encoded template that can be visualized with various fluorescence labeling dyes for barcode recognition purpose, and, hence, multiplex detection of biomolecules was achieved. Regarding that each protein nanofibril represents a single detection platform, a large number of single fibrils simultaneously are monitored with the dual-color TIRFM in a high-throughput manner.

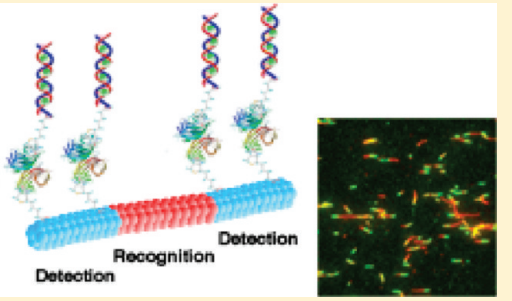

Knowing that a variety of biomolecules play vital roles in triggering diseases, the development of simple but ultrasensitive detection assay for precise profiling of biomolecules, such as proteins, nucleic acids, or cytokines, is in great demand. Because of the low abundance of biomolecules in biological fluid, detection of biomarkers is always challenging. Large amounts of biological samples or multistep sample pretreatment methods are adapted, for the purpose of detecting sufficient signals by the typical spectroscopic instruments. However, these approaches are costly, labor-intensive, and accompanied with sample loss. Lately, in the era of nanotechnology, scientists have developed novel nanomaterials such as metallic nanowires[1−3] and particle-based suspensions[4−6] to serve as a platform for biomarker sensing. These novel biosensing platforms allow the detection of sample with high throughput, as well as minimal assay time, sample volume, and cost. Nevertheless, fabrication of these nanomaterials requires advanced chemical synthetic procedures and careful control in experimental parameters (e.g., material compositions, electroplating conditions, etc.).[7] On the other hand, in order to allow simultaneous detection of several analytes, an encoding scheme for molecular identification is also introduced for sensor recognition;[2,3,8−11] yet, complicated and only limited number of analyte-specific codes are yielded.[12] Hence, a nanoscale substrate that can be fabricated easily and controllably, encoded and functionalized with a variety of biomolecular probes for high throughput and multiplexed detection of biomarkers, is currently desired. Hereby, biological nano materials that are synthesized under ambient conditions are regarded as potential substitutes to the hard matter.

Molecular self-assembly (MSA) is a notable approach for fabricating novel supramolecular architectures.[13,14] Biomolecules including peptides and proteins usually undergo self-assembly process and efficiently form stable, highly reproducible, and well-defined nanostructures with certain functionality under ambient conditions.[7,15,16] Familiar examples of MSA included hexamer formation of insulin,[17] polymeric filament formation of actin,[18] misfolding of proteins into well-ordered fibrillar amyloid,[19] etc.[20] Recently, several groups enforced the prospective bionanotechnological application of peptide-based MSA on signal amplification,[19] biomolecular recognition,[21,22] bionanotransportation,[23] lithographic patterning,[24] etc. Monomeric peptides served as the building block of the architects and were engineered with various functional groups such as fluorophores,[25] biotin,[21] enzymes[19,26] and others to achieve specific purposes. These reports illustrated the potential of peptide-based nanostructures as functional biocompatible multivalent scaffolds for biomarkers detection.

Herein, we developed functionalized self-assembling protein nanofibrils as highly sensitive miniaturized platform for the detection of biomolecules with the aid of fluorescence microscopy. Beta-amyloid (1−40) peptides (Aβ_{1-40}) were taken as a model of the self-assembling protein nanostructure in this work. Aβ_{1-40} forms insoluble fibrous protein aggregates by changing conformation of its secondary structures from native α-helix to cross-β-sheet and stacking into fibrils under physiological

Received: July 29, 2011
Accepted: November 1, 2011
Published: November 01, 2011

conditions.[27] The fabrication of the Aβ fibril is so simple that requires only incubation of monomeric Aβ at 37 °C in phosphate buffer (pH 7.4) over sufficient time (1 h under seed-mediated condition). Co-incubating functionalized and native Aβ monomer converted the ordinary nanofibrils into functional one-dimensional (1-D) protein fibrillar scaffolds and facilitated conjugation of specific probes for precise and ultrasensitive biomolecular detection at subattomole level (with an estimated detection limit of 183 fM in 10 μL of sample solution). Furthermore, an encoding scheme was introduced in our developed assay such that the simultaneous detection of multiple analytes in a single sample could be accomplished. Multifunctional and segmented protein nanofibrils were generated based on self-assembling mechanism of $A\beta_{1-40}$. The as-synthesized protein co-fibrils possessed barcode property and could be visualized and identified with dual fluorescence labeling. Therefore, distinct molecular probes tagged on each protein nanofibrils could be easily distinguished. Regarding that each individual protein nanofibril represented a single detection platform, monitoring a large number of single nanofibril simultaneously with the aid of single-molecule detection technique offered high throughput of the detection system, while the encoding elements increased the detection multiplexity.

EXPERIMENTAL SECTION

Preparation of Cover Glasses. All coverslips were prewashed prior to experiments. Briefly, No.1 22 × 22 square mm cover glasses (Corning, NY) were successively sonicated in absolute ethanol for 5 min, sodium hydroxide (NaOH) solution for 40 min, glacial acetic acid for 15 min, distilled water for 5 min (thrice), and absolute ethanol for 5 min (thrice). Between each solvent replacement, the coverslips were rinsed thoroughly with distilled water. The cleaned coverslips were dried completely at 140 °C oven for ∼15 min and stored for future usage.

Preparation of $A\beta_{1-40}$ Fibrils for Seeding. Monomeric $A\beta_{1-40}$ (Invitrogen) was used without further purification. The stock $A\beta_{1-40}$ was prepared by dissolving 1 mg of $A\beta_{1-40}$ monomers in 400 μL ice-cold 0.02% ammonia solution and stored at −80 °C until use. Fifty microliters (50 μL) of stock solution was diluted to 50 μM with phosphate buffer (50 mM sodium phosphate, 100 mM sodium chloride, pH 7.4). The mixture was incubated in water bath at 37 °C with gentle shaking for 20 h, and stored at −18 °C afterward. Aliquot of stock fibrils was used for the second generation of Aβ seedings. In general, stock fibrils were sonicated for 5 s thrice in order to break them apart into small fragmented fibrils. In consequence, 2 μL of the as-prepared fibrils were added into 5 μL of monomeric $A\beta_{1-40}$ and diluted to 50 μL with phosphate buffer solution. The mixture was incubated at 37 °C for 1 h. The resultant fibrils were sonicated for 5 s thrice and used as the second generation of seedings for the seed-mediated fibrillation.

Preparation of Biotinylated $A\beta_{1-40}$ Fibrils. Stock Biotin-$A\beta_{1-40}$ monomers (Anaspec, CA) were diluted with 0.02% ammonia solution to 100 μM. Biotinylated $A\beta_{1-40}$ fibrils were then prepared by mixing monomeric biotin-$A\beta_{1-40}$ and $A\beta_{1-40}$ in a molar ratio ranged from 1:1 to 1:50, respectively, with a total Aβ concentration of 50 μM. In order to accelerate the fibrillation rate, 0.87 μg/mL of prepared $A\beta_{1-40}$ seeding was added to the solution. The peptide mixture was then incubated at 37 °C for 60 min. The as-prepared fibrils were diluted to appropriate concentration with phosphate buffer prior to experiments.

Preparation of Encoded Multifunctional Biotinylated $A\beta_{1-40}$ Fibrils. Stock Fluorophore-tagged $A\beta_{1-40}$ monomers (F-$A\beta_{1-40}$, where F = TAMRA or FAM, Anaspec) were diluted with 0.02% ammonia solution to 100 μM. F-$A\beta_{1-40}$ fibrils were then prepared by mixing monomeric F-$A\beta_{1-40}$ and $A\beta_{1-40}$ in a molar ratio of 1:4, with a total Aβ concentration of 50 μM. Seeds were added into the mixture solution and was then incubated at 37 °C for 1 h. Consequently, 100 μM $A\beta_{1-40}$ monomer and 100 μM biotinylated $A\beta_{1-40}$ monomer was added into the as-prepared F-Aβ fibrils, respectively (v/v/v 1:1:10), and incubated at 37 °C for 1 h. Resulting fibrils were diluted to appropriate concentration with phosphate buffer prior to experiments.

Immobilization of Amyloid Fibrils on the Surface of Flow Cell. Here, sealed flow cell was prepared by combining two precleaned cover glasses with double-sided adhesive tapes with a channel width of ∼3 mm each. Successively, 10 μL of diluted amyloid fibrils and 1× phosphate buffer solution was flowed into the flow cell, respectively. Solutions in excess were withdrawn at the outlet with Kimwipes, based on capillary force. Fibrils were also stretched under the force of capillary action. For the study of biotin-streptavidin interaction, additional 10 μL of Alexa Fluor 555-labeled streptavidin (AF555-Stv, Invitrogen) solutions of appropriate concentration was flowed into the channel after the flow of phosphate buffer and PBS buffer with 1% of bovine serum albumin (PBS-1% BSA, which minimize nonspecific adsorption of AF555-Stv on glass slides), and consequently incubated at room temperature for 30 min before imaging. The flow cell was placed under the home-built prism-type total internal reflection fluorescence (TIRFM) system for imaging with the excitation of a 532-nm laser for the study of AF555-Stv conjugation on biotinylated fibrils

Detection of DNA Sequences with Biotinylated $A\beta_{1-40}$ Fibrils. In the detection of DNA sequences with biotinylated fibrils, fibrils were first immobilized on the flow cell as mentioned previously. Excess streptavidin (Stv, Sigma−Aldrich)/AF555-Stv mixture (molar ratio of 2:1) were then added into the channel, incubated for 15 min, and was then successively washed with phosphate buffer and PBS buffer with 1% of bovine serum albumin (BSA, Sigma). AF555-Stv was added for localization of fibrils in the images. Consequently, excess biotinylated-poly-$(T)_{15}$ probe (5′-biotin-TTT TTT TTT TTT TTT-3′, Invitrogen, HPLC-purified, same for all sequences mentioned hereafter) were added into the channel and incubated for 15 min to saturate the available Stv sites. Afterward, the channel was washed with phosphate buffer. Target poly$(A)_{15}$ (5′-AAA AAA AAA AAA AAA-3′) of 250, 100, 50, 10, 5, 1, 0.5, 0.1, 0.05, and 0 pM (blank) were added into the channel, hybridized for 30 min at room temperature for detection and calibration, respectively. For negative control experiments, poly$(G)_{15}$ (5′-GGG GGG GGG GGG GGG) was used to demonstrate the selectivity of the sensor. YOYO-1 iodide (YOYO, Invitrogen) was finally added to label and produce fluorescence signals from the hybridized DNA duplex. The flow cell was placed under the home-built prism-type total internal reflection fluorescence (TIRFM) system for imaging with the excitation of a 488-nm laser.

Detection of DNA Sequences with Encoded $A\beta_{1-40}$ Fibrils. In the detection of DNA sequences by the encoded fibrillar sensor, an approach similar to that of the monofunctional one was applied. In general, solution was added into the channel in the following order: (i) biotin/TAMRA/biotin (BTB) fibrils, PBS-1% BSA, 500 nM Stv, 500 nM biotinylated poly$(T)_{15}$ probe, 500 pM poly$(A)_{15}$ target, 20 nM YOYO; and (ii)

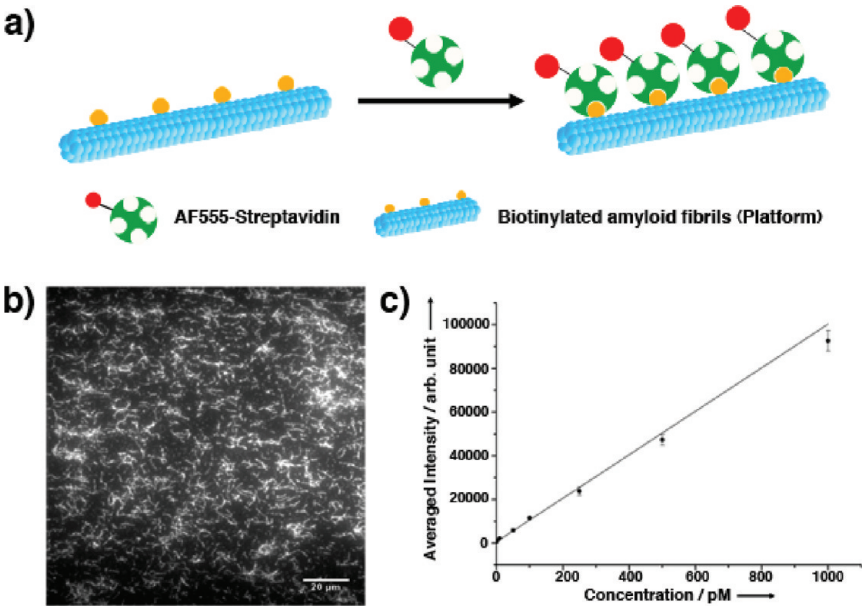

Figure 1. (a) Detection scheme of Alexa Fluor 555-Streptavidin by biotinylated Aβ fibrillar platform. (b) Fluorescence image of biotinylated Aβ excited at 532 nm. Fluorescence signals come from the AF555-Stv molecules (500 pM) conjugated along the fibrils. (c) The calibration curve demonstrates the linear relationship between integrated fluorescence intensity from the biosensors and the concentration of target AF555-Stv molecules. R^2 = 0.9998. Error bars, standard error of mean, n = 3.

biotin/FAM/biotin (BFB) fibrils, PBS-1% BSA, 500 nM Stv/AFStv (molar ratio 10:1), biotinylated poly(T)$_{15}$ probe, 500 pM poly(A)$_{15}$ target, 20 nM YOYO. Phosphate buffer was added between each addition before hybridization of DNA in order to remove excess components within the channel. The flow cell was incubated at room temperature to allow hybridization of DNA sequences after the addition of target DNA sequences. The resulting flow cell was placed under the TIRFM system for imaging with the excitation of 532-nm and 488-nm lasers, respectively, for dual-color fluorescence imaging.

Total Internal Reflection Fluorescence Microscopy (TIRFM) Imaging System. An inverted Model IX-71 microscope (Olympus, Tokyo, Japan) was equipped with a high-numerical-aperture 60× (1.45 NA) oil-immersion objective (PlanApo, Olympus). The sample coverslip was located between the fused-silica Isosceles Brewster Prism (CVI Melles Griot, Carksvadm, CA) and the 60× objectives with immersion oil (n = 1.52, Nonfluorescence, Olympus). For the fluorescence excitation, a 445-nm diode laser (50 mW, LQC445-40E, Newport, USA) was used for the excitation of thioflavin T (ThT) labeled Aβ_{1-40}, while a 488-nm cyan laser (50 mW, CMA1-01983, Newport, NJ) was used for the excitation of FAM-Aβ_{1-40} and YOYO and a 532-nm laser (125 mW, DPGL-2100F, Photop) were used for the excitation of TAMRA-Aβ_{1-40} and AF555-Stv conjugate were used in the experiments, respectively. The incident angle of the laser beam was adjusted to 66° in order to achieve the total internal reflection (TIR) and generates evanescent field for the excitation of the fluorophores. Three types of band-pass filters—HQ 480/40x (Chroma Technology Corp., USA), HQ 535/50 (Chroma), and HQ 610/75 (Chroma)—were coordinated with the use of 445-, 488-, and 532-nm laser excitation in the imaging, correspondingly. Fluorescence images were captured by an electron-multiplying charge-coupled device (EMCCD) camera (PhotonMax 512, Princeton Instruments, Princeton, NJ, USA) incorporated with a Uniphase mechanical shutter (Model LS2Z2, Vincent Associates, Rochester, NY) and a driver (Model VMM-T1, Vincent Associates) in external synchronization mode and frame-transfer mode. The exposure time of both the camera and the shutter driver were set at 100 ms, while the multiplication gain of the camera and the delay of the driver was set at 4000 and 100 ms, respectively. Images were obtained with the WinSpec/32 software (Version 2.5.22.0, Downingtown, PA) provided by Princeton Instruments. In general, 10 consequent images were accumulated in each condition in order to provide sufficient fluorescent signals for further data processing.

Data Analysis. All data analysis was performed with the use of a public-domain image processing software, ImageJ. The lengths of fibrils were determined manually. In general, the length of fibrils was outlined with the Freehand Drawing function of ImageJ. The length of fibrils was automatically defined with the Measure function. One hundred fibrils were measured for each independent experiment. Average length of fibrils in each condition was determined by fitting the Gaussian distribution of length of 100 fibrils with the OriginPro8 software. Fluorescent signals of fibrillar sensors were determined by measuring the net intensity of 30 randomly located region of interest (ROI) with an area of 15 × 2 square pixels on fluorescent fibrils in each condition with ImageJ. Net intensity = 30 × (15 × 2 square pixels of independent fluorescent area on fibrils) − 30 × (15 × 2 square pixels of independent background area on image). Three independent experiments were performed for each condition, while the mean of mean and the standard error of the mean (S.E.M.) among the result from the triplicates was taken for the plot, unless specified.

RESULTS AND DISCUSSION

Since the behavior of amyloid is highly dependent on conformation of peptide monomer, it is noteworthy to emphasize that, in the preparation of functionalized Aβ fibrils, some

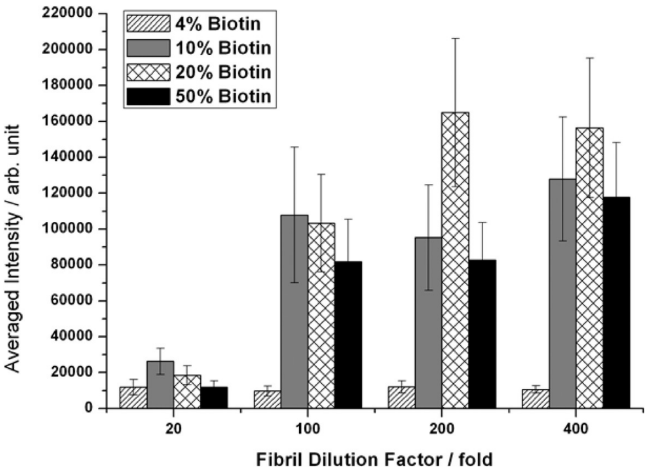

Figure 2. Optimization of the sensitivity of nanofibrillar sensor. Fluorescence intensity of 1 nM AF555-Stv that is conjugated on biotinylated Aβ fibrils was measured. The fibrillar sensors were prepared by incubating 4%, 10%, 20%, and 50% of biotinylated-Aβ monomers with native monomer in a total Aβ concentration of 50 μM, respectively, and were also immobilized on the glass slides with different fibril density (20×, 100×, 200×, and 400× dilution) respectively. Error bar, standard deviation. n = 30 (with a selected region-of-interest of 15 × 2 square pixels on a fibrillar sensor).

functional residues might kinetically or sterically interfere with the self-assembly process and obstruct the formation of nanofibrillar structures.[25] We co-incubated different molar ratios of biotinylated and native Aβ_{1-40} monomers (with a total [Aβ_{1-40}] = 50 μM) for an hour under physiological conditions, respectively. The as-prepared fibrils were injected into a flow cell, stretched and electrostatically adhered onto the surface of the glass slides, labeled with fluorescence dye Thioflavin T (ThT, λ_{ex} = 450 nm, λ_{em}= 482 nm), and monitored directly with prism-type total internal reflection fluorescence microscopy (TIRFM) coupled with EMCCD camera for detection. It was revealed that the average length of the fibrils was shorter when there was a higher percentage of biotinylated monomer presented among the total monomer solution and vice versa (see Figure S1 in the Supporting Information). For instance, the average length of fibrils incubated from Aβ_{1-40} monomers containing 50%, 10%, and 0% (control) biotinylated Aβ_{1-40} were 6.3 ± 0.2, 7.3 ± 0.1, and 9.2 ± 0.1 μm, respectively. The results agreed with the previous report that shorter fibrils would be yielded in the presence of N-terminal labeled Aβ monomer, because of the change in morphology of the peptide.[25] This phenomenon, alternatively, also provided evidence that the extent of amyloid fibrillation could be simply regulated by varying the ratio of functionalized monomer among the total monomeric peptide solutions.

The activity of the biotinylated amyloid fibrils was confirmed by the strong biotin-streptavidin interaction. In principle, different concentrations of Alexa Fluor 555-tagged streptavidin (AF555-Stv, λ_{ex} = 555 nm, λ_{em} = 565 nm) were added into the homemade flow cell (see Figure S2 in the Supporting Information) and interacted with the biotinylated amyloid fibrils. Because of the strong binding affinity of the biotin and streptavidin (Stv) molecules, AF555-Stv conjugated onto the biotinylated fibrils and fluoresced (see Figure 1a). With the evidence of the TIRFM images, we observed that (i) fibrillar structures were visualized under the excitation of a 532-nm laser (Figure 1b); and

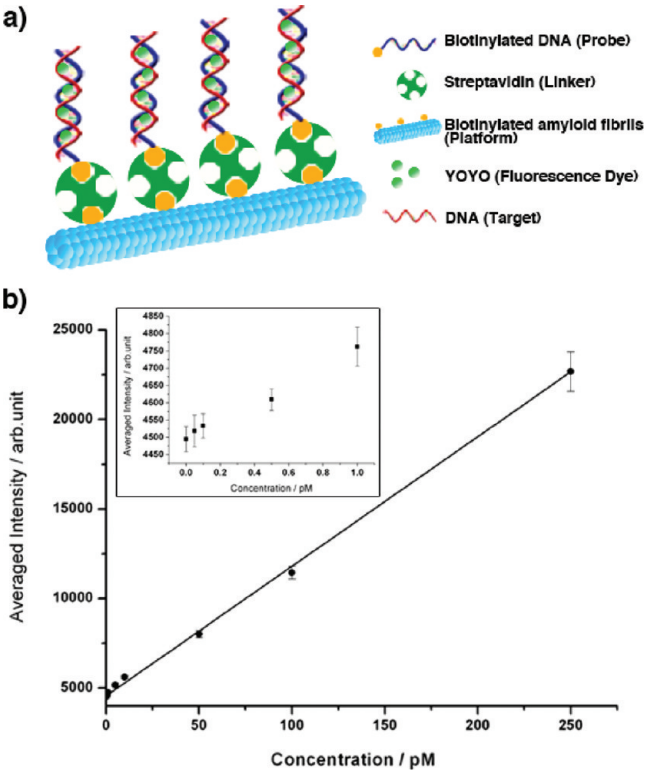

Figure 3. (a) Detection scheme of poly(A)$_{15}$ by DNA probe conjugated biotinylated Aβ fibrillar platform. (b) Calibration curve showing the linear relationship between averaged fluorescence intensity generated from YOYO-intercalated DNA hybrids and the concentration of target poly(A)$_{15}$. R^2 = 0.9989. Detection limit of the assay is 183 fM. Inset in panel (b) shows a magnified region of the calibration curve (ranging from 0 to 1 pM). Error bars, standard error of mean, n = 3.

(ii) a linear correlation was obtained between the fluorescence intensity of the fibrils and the concentration of the AF555-Stv added (Figure 1c). The results supported that the biotin moiety on the Aβ fibrils was actively functioning. Furthermore, the linear relationship established between the fluorescence signals and concentration of AF555-Stv showed that the self-assembling protein nanofibril is a competent protein (streptavidin) detector.

The nanofibrillar platform actually operated as an online preconcentrator and also a signal enhancer in this biomolecular detection assay. In solution-based single molecule detection (SMD), fluorescence analyte diffuses randomly within the detection volume and thus the generated signals are relatively dispersed and weak. Although the situation can be improved by immobilizing the molecular probes onto the surface of cover glasses, such that most of the fluorophores can be trapped on the surface and excited by the evanescent field generated by total internal reflection, the efficiency of immobilization may restrain the density and activity of the probes and, hence, affect the sensitivity of the detection assay. In contrast, a nanofibrillar platform entrapped all freely diffusing analytes onto a well-defined nanoscale region, thus producing strong "line-form" fluorescence signals. The detection limit of the detection assay was thus greatly improved. Practically, the sensitivity of the developed sensor, besides the fluorescence signals generated by the labeling dye, was also highly dependent on two factors: (i) the percentage of biotin groups on the fibrils, and (ii) the density (number) of the fibrils (sensors) on the slide. Biotin moiety, as the linker

dx.doi.org/10.1021/ac2019602 |Anal. Chem. 2011, 83, 9370–9377

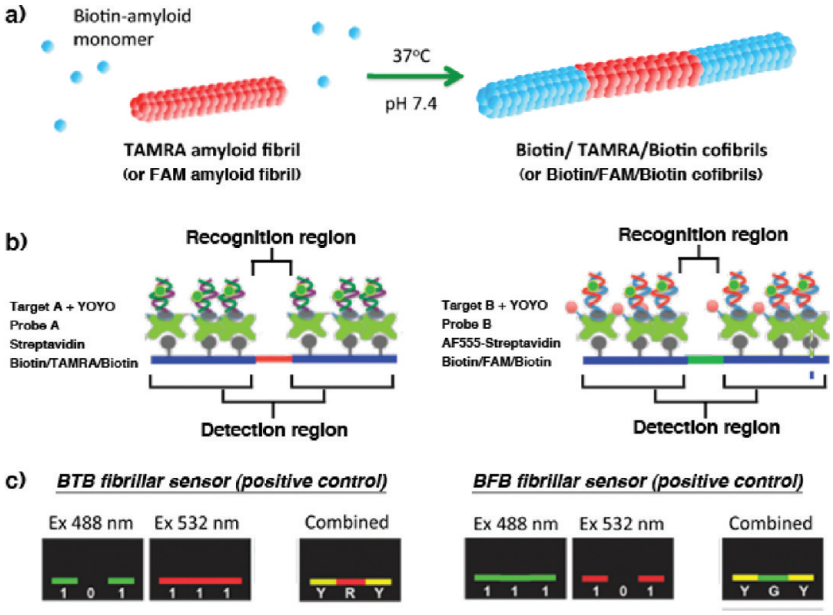

Figure 4. (a) Preparation of three-segment multifunctional Aβ fibrils with functional patterns of biotin/TAMRA/biotin. (b) Encoded multifunctional nanofibrillar sensors BTB fibrils and BFB fibrils applied in the detection of distinctive DNA sequences simultaneously. Central fluorophore serves as the recognition region while the biotin on the two end terminals serve as the detection region. The biotin moiety is conjugated with streptavidin linker and biotinylated DNA probes in order to capture target DNA molecules. YOYO dye is added to label the hybridized DNA duplexes. (c) Expected emission color schemes and virtual color of the fluorescence images for BTB fibrils (left) and BFB fibrils (right) were shown. YOYO and FAM would switch on, under 488-nm excitation, while TAMRA and AF555-Stv would switch on under 532-nm excitation.

between the detection platform (fibril) and the biomolecular probe, critically governed the capturing efficiency of the target analyte. Diminution of biotins on fibrils, and consequently, in conjugated probes, would eventually minimize the detection capacity of the sensor as number of capturing sites was reduced. On the other hand, the high number of fibrils on the slides, although improved the throughput of the detection, might dilute the signals from a pool of analyte molecules by distributing themselves among higher number of fibrils. Therefore, optimization on the percentage of biotin groups on fibrils and the density of fibrils in detection volume is necessary.

Figure 2 shows the optimization of the detection sensitivity of the nanofibrillar sensors. It was noted that a higher percentage of biotinylated amyloid, with respect to native amyloid, in fibrils would generally yield better signals when 1 nM of AF555-Stv was added into the sensors. Herein, 20% of biotinylated amyloid gave the strongest fluorescence signals among all. An increase in biotin composition to 50%, however, did not further increase the signals. On the other hand, the detection signals were greatly improved when the density of immobilized fibrils on the slides decreased from 20-fold dilution to 200-fold dilution, which agreed with our hypothesis that signals from analyte may be "diluted" among a high number of sensors. Besides, a diminished trend in fluorescence signals was observed when the dilution factor increased from 200-fold to 400-fold. We accounted that some analytes cannot be trapped during the sampling time by the limited amount of sensors when the fibril density was significantly reduced, and, hence, a portion of the signals was lost. Hereafter, we took 200× diluted biotinylated fibrils with 20% of biotinylated amyloid as the optimal platform for biomarker detection.

As a proof of concept, we hereby applied the well-optimized protein nanofibril platform in the detection of short DNA sequences. Poly$(A)_{15}$ was chosen as an example to be detected by the platform, as shown in Figure 3a. In general, biotinylated-poly$(T)_{15}$ was adopted as the detection probe and was conjugated with the biotinylated Aβ fibrils by streptavidin linkers. BSA was applied into the flow cell channel in order to minimize any nonspecific adsorption of biomolecules onto the slide surface. In order to validate the performance of the detection platform, different concentrations of target poly$(A)_{15}$, with a sample volume of 10 μL each, were added into the flow cell channels and hybridized at optimal temperature respectively. Finally, the DNA bis-intercalating dye YOYO-1 iodide (YOYO, λ_{ex} = 491 nm, λ_{em} = 509 nm) was flowed in to label the hybridized DNA duplex in a dye to base-pair ratio of 1:1. Since free YOYO has a low quantum yield (QY), and it has a low affinity toward single-stranded DNA, post-treatment wash of excessive dyes is not necessary. Hence, this fibrillar sensor assay is wash-free. The resultant fibrils with sandwich detection layer were visualized under the TIRFM system with the excitation of a 488-nm laser. Emitted fluorescence intensity is correlated to the quantity of hybrids formed, which, in turn, is the quantity of the target DNA. Figure S3 in the Supporting Information shows the typical TIRFM images of the nanofibril sensor with target analyte. In the image, each fibrillar structure was an independent biosensor. Simultaneous observation of numerous fibrils offered high-throughput detection. Intensity signals of 30 sensors were measured and averaged in each trial for calibration purpose. A calibration curve with a high linearity of R^2 = 0.9989 was established (see Figure 3b) and a theoretically calculated limit of detection (LOD) of 183 fM was achieved (LOD = mean of blank + (3 × standard error of mean of blank)). In the control experiments, poly$(G)_{15}$ was applied to demonstrate the selectivity of our amyloid sensor. It was observed that the fluorescence signals obtained from the detection of 250 pM poly$(G)_{15}$ were

dx.doi.org/10.1021/ac2019602 |*Anal. Chem.* 2011, 83, 9370–9377

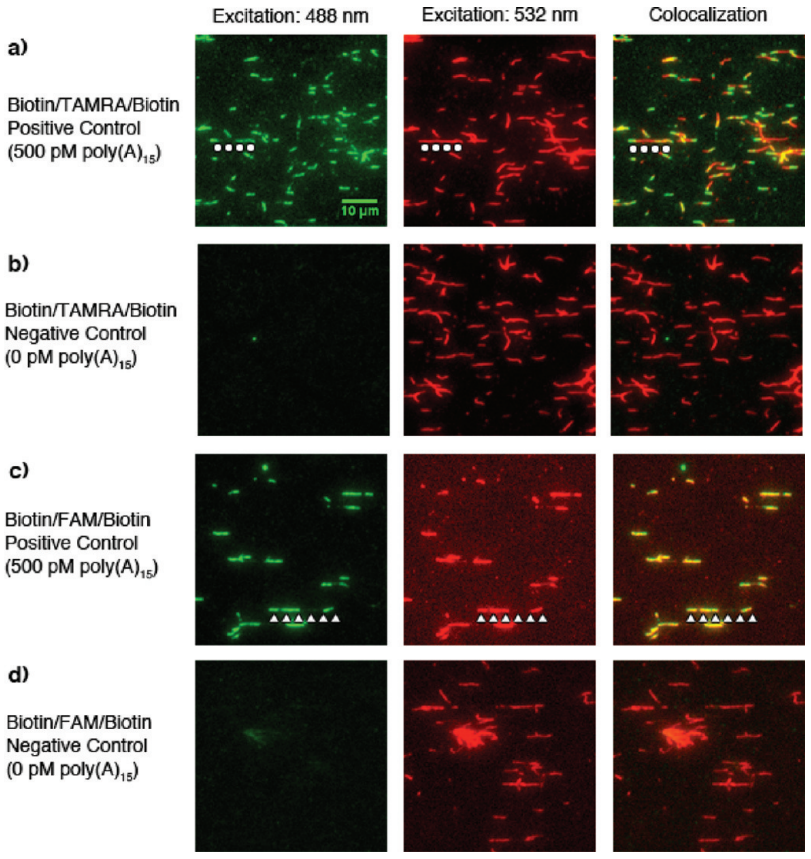

Figure 5. Selected region of fluorescence images of the BTB (panels (a) and (b)) and BFB (panels (c) and (d)) nanofibrillar sensors in the presence (panels (a) and (c)) and absence (panels (b) and (d)) of DNA targets. Representative images of the fluorescence emission excited by 488-nm emission (left), 532-nm emission (middle), and the co-localized emission (right) are shown for each condition. Three-segment yellow/red/yellow (denoted by white circles, ○) and yellow/green/yellow (denoted by white triangles, △) patterns were observed in the co-localization image of BTB and BFB fibrils in the positive control (panels (a) and (c)) respectively, however, was not observed in the negative control (panels (b) and (d)), showing that the encoded pattern is specific to the presence of target DNA sequences.

significantly lower than that of target poly(A)$_{15}$ of the same concentration, and were comparable to the blank (see Figure S4 in the Supporting Information). These results supported that the nature of our nanofibrillar sensor is high throughput, high precision, high selectivity, and ultrahigh sensitivity.

To address the need for multiplex biomolecular detection as mentioned previously, an encoding scheme using our self-assembled protein nanofibrils was introduced, such that molecular recognition can be achieved. As proposed by Walsh et al., one of the possible mechanisms of Aβ fibrillogenesis is the end-to-end annealing of Aβ monomers.[28] Accordingly, freshly added monomer would attach to the two ends of the preformed nucleus/protofibrils and be further extended into the fibrillar structure. Based on this hypothesis and evidence from some other relevant reports,[18,29] we expected that the addition of fresh biotinylated Aβ_{1-40} monomers into as-prepared fluorophores-tagged Aβ fibrils might become multifunctional Aβ fibrils with alternate-segmented patterning (i.e., biotin/fluorophores/biotin). As a proof of concept, we fabricated three-segment multifunctional Aβ fibrils by incubating biotinylated Aβ_{1-40} monomers with preformed fluorophore (FAM, λ_{ex} = 492 nm, λ_{em}= 518 nm or TAMRA, λ_{ex} = 541 nm, λ_{em} = 568 nm)-tagged Aβ_{1-40} fibrils for 1 h under physiological conditions. Figure 4a shows the proposed mechanism of the fabrication of three-segment biotin/FAM/biotin (BFB) and biotin/TAMRA/biotin (BTB) Aβ fibrils. The as-formed three-segment fibrils were bifunctional in nature: (i) detection region for specific target biomolecules with the biotinylated segment at two ends of the fibrils, and (ii) recognition region with the central part of the fibrils tagged with fluorophores (e.g., FAM and TAMRA) of distinguishable fluorescence excitation and emission wavelengths when detected by dual-color fluorescence microscopy.

The encoded Aβ fibrils are more advantageous than typical metallic striped nanowires, in terms of simplicity and flexibility in fabrication. It is because functionalized Aβ monomers are widely available and protein functionalization techniques are well-established. In principle, many different combinations of analyte-specific codes can be generated in our encoded fibrils system by (i) using the fluorophores with other substitutes of different excitation and emission wavelengths in the recognition region; (ii) replacing the fluorophores with other functional groups, such as $-NH_2$, $-COOH$, $-SH$, etc., for conjugation of other materials that could provide specific identification properties (e.g., metallization of fibrils[30,31] or tagging with nanoparticles[21]) in the recognition region; and (iii) reversing the positions between the recognition and detection regions located on the protein fibrils (i.e., fluorophores/biotin/fluorophores). By conjugating various molecular probes onto segment of each multifunctional fibrils of unique pattern, simultaneous assays of multiple analytes are promising.

dx.doi.org/10.1021/ac2019602 |*Anal. Chem.* 2011, 83, 9370–9377

Hereby, we demonstrated the schematic and proposing color-coding scheme of the three-segment encoded Aβ fibrillar platforms, BTB and BFB, as shown in Figures 4b and 4c, for the detection of DNA sequences. The detection principle of the encoded functional sensor was identical to that of monofunctional fibrillar sensor as described previously, except that streptavidin linker was replaced with a mixture of Stv/AF555-Stv in the BFB fibrillar assay for better recognition. Because of the difference in maximum excitation wavelength, fluorophores would only be switched on at appropriate excitation wavelength under dual-color TIRFM (in general, 488 nm for FAM and YOYO, and 532 nm for TAMRA and AF555-Stv). In the fluorescence images (Figure 5), virtual colors were adapted for better clarification due to the monochromic nature of the EMCCD camera. For instance, in the presence of target DNA, which hybridized with the corresponding probe on the BTB fibrils and was labeled with YOYO, the fluorescence images displayed the emission of the YOYO at the two ends of the fibrils (Figure 5a, left panel, λ_{ex} = 488 nm, green), and TAMRA in the middle of the fibrils (Figure 5a, middle panel, λ_{ex} = 532 nm, red) at two separate excitation wavelengths. The two end terminals of the BTB fibrils that were expected to be silent under the 532-nm excitation, however, were found in low intensity in red. Herein, the weak red emission from the end terminals was actually originated from the trace amount of TAMRA-Aβ_{1-40} that was mixed with the native and biotinylated-mAβ during the fabrication of three-segment fibrils. Nonetheless, this phenomenon did not interfere with the detection and recognition properties of the encoded sensor. Merging the two images revealed the three-segment patterns of yellow/red/yellow (Figure 5a, right), in which the detection region was displayed as yellow at the two ends of the fibrils for the presence of both YOYO (green) and trace TAMRA (red), while the central recognition region was red for the presence of TAMRA. The resulted images in Figure 5a agree well with our proposed color-coding scheme (Figure 4c), showing that the three-segmented BTB fibrillar detection assay was encoded under dual-color TIRFM for target DNA. Similar schemes and images were also illustrated in Figures 4c and 5c for the BFB fibrillar sensor. A three-segment pattern of yellow/green/yellow, as proposed, was also successfully obtained when target DNA sequence was being detected by the complementary probes that were conjugated on the BFB fibrils. Figures 5b and 5d show the negative control of the BTB and BFB detection assays, respectively. In the absence of target DNA strands, no encoded pattern of both BTB and BFB fibrils were observed. Herein, only free and single-strand DNA-bounded YOYO was being excited under 488-nm excitation and, therefore, a very low fluorescence signal (background) resulted. As the emission color codes of the BTB (yellow/red/yellow) and BFB (yellow/green/yellow) fibrils in the presence and absence of analytes were clearly differentiable, detection of multiple species could be achieved in parallel and multiplexed detection is promised. In short, these novel encoded fibrillar sensors can detect DNA both (i) qualitatively, by monitoring the existence of encoded segments (i.e., multiple segments if positive, but single segment if negative); and (ii) quantitatively, by measuring the corresponding fluorescence signals in the detection region of the encoded three-segment fibrils, respectively.

CONCLUSIONS

In conclusion, functionalized self-assembling protein nanofibrils platform for the detection of biomolecules with high sensitivity and high throughput in miniature scale was developed. The preparation of the protein nanofibrils was simple and direct, in which the peptide monomers self-assemble into fibrillar structure under physiological conditions within an hour, and the as-prepared fibrils would electrostatically adhere on the surface of the glass slides spontaneously such that chemical modification and surface treatment to glass slides was unnecessary prior to experiment. An encoding scheme was introduced by preparing three-segment multifunctional protein cofibrils in order to allow multiplexed screening of biomolecules in parallel, using dual-color fluorescence microscopy. In order to improve the selectivity, the DNA probe demonstrated in this article can be substituted with locked nucleic acid (LNA) or peptide nucleic acid (PNA) that possesses better thermostability in order to enhance the detection performance of the assay, especially in terms of single-base mismatch discrimination. Furthermore, there are numerous flexible modification possibilities available in our proposed assays. One can apply not only the Aβ_{1-40} peptides but also other self-assembling proteins, such as actin and collagen, of different morphologies and functionalizations that can govern the lengths, functional compositions, and bring multifarious encoding patterns to the biomaterial platforms. In addition, biomolecules, like antibodies or protein receptors, can be used instead of DNA to transform the "DNA-nanoarray" into a miniature immunosorbent assay or platform for molecular-level studies. This work provides valuable insights in the application and development of bionanomaterials in the study of biomolecules.

ASSOCIATED CONTENT

Supporting Information. Length distribution of biotinylated-Aβ fibrils prepared with different ratios of free/biotin Aβ monomers, schematic representation of the flow cell, TIRFM images of biotinylated-Aβ fibrils detecting DNA of different concentrations and target selectivity of the amyloid sensors. (PDF) This material is available free of charge via the Internet at http://pubs.acs.org.

AUTHOR INFORMATION

Corresponding Author
*Fax: (+852) 3411-7348. E-mail: hwli@hkbu.edu.hk.

ACKNOWLEDGMENT

This work was fully supported by the Research Grant Council of the Hong Kong Special Administrative Region, P. R. China (HKBU201309) and Faculty Research Grant of the Hong Kong Baptist University (FRG2/10-11/033). We thank Dr. Kai-Ming Yeung for helpful discussion.

REFERENCES

(1) Nicewarner-Pena, S. R.; Freeman, R. G.; Reiss, B. D.; He, L.; Pena, D. J.; Walton, I. D.; Cromer, R.; Keating, C. D.; Natan, M. J. *Science* **2001**, *294*, 137–141.

(2) Stoermer, R. L.; Cederquist, K. B.; McFarland, S. K.; Sha, M. Y.; Penn, S. G.; Keating, C. D. *J. Am. Chem. Soc.* **2006**, *128*, 16892–16903.

(3) Tok, J. B. H.; Chuang, F. Y. S.; Kao, M. C.; Rose, K. A.; Pannu, S. S.; Sha, M. Y.; Chakarova, G.; Penn, S. G.; Dougherty, G. M. *Angew. Chem., Int. Ed.* **2006**, *45*, 6900–6904.

(4) Wu, C. F.; Schneider, T.; Zeigler, M.; Yu, J. B.; Schiro, P. G.; Burnham, D. R.; McNeill, J. D.; Chiu, D. T. *J. Am. Chem. Soc.* **2010**, *132*, 15410–15417.

(5) Cunin, F.; Schmedake, T. A.; Link, J. R.; Li, Y. Y.; Koh, J.; Bhatia, S. N.; Sailor, M. J. *Nat. Mater.* **2002**, *1*, 39–41.
(6) Fenniri, H.; Chun, S.; Ding, L. H.; Zyrianov, Y.; Hallenga, K. *J. Am. Chem. Soc.* **2003**, *125*, 10546–10560.
(7) Gao, X. Y.; Matsui, H. *Adv. Mater.* **2005**, *17*, 2037–2050.
(8) Finkel, N. H.; Lou, X. H.; Wang, C. Y.; He, L. *Anal. Chem.* **2004**, *76*, 353A–359A.
(9) Hartgerink, J. D.; Beniash, E.; Stupp, S. I. *Science* **2001**, *294*, 1684–1688.
(10) Hernandez, R. M.; Richter, L.; Semancik, S.; Stranick, S.; Mallouk, T. E. *Chem. Mater.* **2004**, *16*, 3431–3438.
(11) Han, M. Y.; Gao, X. H.; Su, J. Z.; Nie, S. *Nat. Biotechnol.* **2001**, *19*, 631–635.
(12) Pregibon, D. C.; Toner, M.; Doyle, P. S. *Science* **2007**, *315*, 1393–1396.
(13) Whitesides, G. M.; Boncheva, M. *Proc. Natl. Acad. Sci. U.S.A.* **2002**, *99*, 4769–4774.
(14) Whitesides, G. M.; Mathias, J. P.; Seto, C. T. *Science* **1991**, *254*, 1312−1319.
(15) Niemeyer, C. M. *Angew. Chem., Int. Ed.* **2001**, *40*, 4128–4158.
(16) Zhang, S. G. *Nat. Biotechnol.* **2003**, *21*, 1171–1178.
(17) Brader, M. L.; Dunn, M. F. *Trends Biochem. Sci.* **1991**, *16*, 341–345.
(18) Andrianantoandro, E.; Blanchoin, L.; Sept, D.; McCammon, J. A.; Pollard, T. D. *J. Mol. Biol.* **2001**, *312*, 721–730.
(19) Men, D.; Guo, Y. C.; Zhang, Z. P.; Wei, H. P.; Zhou, Y. F.; Cui, Z. Q.; Liang, X. S.; Li, K.; Leng, Y.; You, X. Y.; Zhang, X. E. *Nano Lett.* **2009**, *9*, 2246–2250.
(20) Kokkoli, E.; Mardilovich, A.; Wedekind, A.; Rexeisen, E. L.; Garg, A.; Craig, J. A. *Soft Matter* **2006**, *2*, 1015–1024.
(21) Kodama, H.; Matsumura, S.; Yamashita, T.; Mihara, H. *Chem. Commun.* **2004**, 2876–2877.
(22) Linse, S.; Cabaleiro-Lago, C.; Xue, W. F.; Lynch, I.; Lindman, S.; Thulin, E.; Radford, S. E.; Dawson, K. A. *Proc. Natl. Acad. Sci. U.S.A.* **2007**, *104*, 8691–8696.
(23) Patolsky, F.; Weizmann, Y.; Willner, I. *Nat. Mater.* **2004**, *3*, 692–695.
(24) Doh, J.; Irvine, D. J. *J. Am. Chem. Soc.* **2004**, *126*, 9170–9171.
(25) Jungbauer, L. M.; Yu, C.; Laxton, K. J.; Ladu, M. J. *J. Mol. Recognit.* **2009**, 403–413.
(26) Leng, Y.; Wei, H. P.; Zhang, Z. P.; Zhou, Y. F.; Deng, J. Y.; Cui, Z. Q.; Men, D.; You, X. Y.; Yu, Z. N.; Luo, M.; Zhang, X. E. *Angew. Chem., Int. Ed.* **2010**, *49*, 7243–7246.
(27) Xu, S. H. *J. Phys. Chem. B* **2009**, *113*, 12447–12455.
(28) Walsh, D. M.; Lomakin, A.; Benedek, G. B.; Condron, M. M.; Teplow, D. B. *J. Biol. Chem.* **1997**, *272*, 22364–22372.
(29) Liang, Y.; Lynn, D. G.; Berland, K. M. *J. Am. Chem. Soc.* **2010**, *132*, 6306–6308.
(30) Wei, G.; Reichert, J.; Jandt, K. D. *Chem. Commun.* **2008**, 3903–3905.
(31) Scheibel, T.; Parthasarathy, R.; Sawicki, G.; Lin, X. M.; Jaeger, H.; Lindquist, S. L. *Proc. Natl. Acad. Sci. U.S.A.* **2003**, *100*, 4527–4532.